Electrospray Mass Spectrometry for Characterizing Polyglycerols and the Effects of Adduct Ion and Cone Voltage

Molly W. Crowther*, Terrence R. O'Connell, and Stephen P. Carter

Lonza, Inc., Annandale, New Jersey 08801

ABSTRACT: Polyglycerol intermediates have been characterized by liquid chromatography–mass spectrometry (LC–MS) with electrospray ionization (ESI). Linear and cyclic components from n = 2–23 in a sample of decaglycerol, for example, have been resolved in the second dimension or mass axis. Molecular weight (MW) distributions for tri-, hexa-, and decaglycerol products have been analyzed as a function of cone voltage and adduct ion (H^+, Li^+, Na^+, K^+, Rb^+, Cs^+, and NH_4^+). A different combination is required to obtain a reliable MW distribution for each polyglycerol intermediate. The best distribution obtained by ESI/MS is determined by comparing the calculated hydroxyl number and cyclic content to that obtained by wet chemistry and gas chromatography, respectively. Once ESI/MS conditions are established, the distribution can be used, for the first time in polyglycerol analysis, to calculate important parameters such as number average MW, weight average MW, polydispersity, % cyclics, hydroxyl number, wt% above n = 6, etc.
JAOCS 75, 1867–1876 (1998).

KEY WORDS: Adduct ion, cone voltage, electrospray ionization, ESI/MS, LC–MS, mass spectrometry, molecular weight, polydispersity, polyglycerol, polymer distribution.

Polyglycerols are intermediates for polyglycerol fatty esters, used as additives in the food and personal-care industries. Knowledge of the polyglycerol distribution will help relate composition to performance, optimize process chemistry, and produce newly tailored products. Gas chromatography (GC) of an acetylated polyglycerol can resolve linear and cyclic components only up to hexad chains (1). Furthermore, the peak intensities in the gas chromatogram are progressively attenuated with increasing degree of polymerization. High-performance liquid-chromatography (HPLC) with refractive index (RI) detection and a carbohydrate column partially resolves polymers up to n = 12, but cyclic and linear components (larger than diglycerol) are not resolved (2). Supercritical fluid chromatography of silanized polyglycerols shows peak maxima up to n = 10. Higher molecular weight (MW) polymers elute, but still not all cyclic and linear components are resolved (3). Liquid chromatography–mass spectrometry (LC–MS) with electrospray ionization (ESI) has advantages compared with all the above techniques since all components are eluted and the linear and cyclic components can be resolved. The observed MW distribution is not only dependent upon the cone voltage but also on the adduct ion used in the analysis. Here, the optimized combination of cone voltage and adduct ion is found by comparing calculated and experimentally determined parameters [hydroxy number (OH#) and percentage of cyclics]. The right combination can give a representative distribution from which important parameters such as M_n (number average MW), M_w (weight average MW), polydispersity, % cyclics, OH#, wt% above n = 6..., can be reliably calculated for the first time in polyglycerol analysis.

Figure 1A shows a general structure of polyglycerol where n is equal to the degree of polymerization. Condensation products can be linear or branched as shown for diglycerol in Figure 1B. In addition, dehydration (intramolecular condensation) can occur and the mono-cyclic components in Figure 1C are also possible. Dicyclic diglycerol components are inconsistent with the proposed synthetic mechanism of an epoxide intermediate. (4,5) The number of possible structures becomes increasingly unwieldy for each additional degree of polymerization. A computer program used by Dolhaine *et al.* (6,7) calculates over 7000 possible structures for a hexaglycerol excluding the stereochemical isomers.

There have been a limited number of applications of ESI/MS for the analysis of MW distributions of synthetic polymers. Prokai and Simonsick, Jr. (8) describe the coupling of gel permeation chromatography with ESI/MS for the

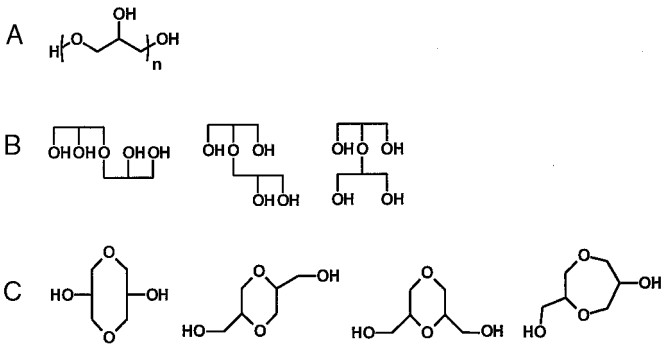

FIG. 1. (A) General structure for polyglycerol. (B) Structures for linear and branched diglycerol. (C) Possible structures for monocyclic diglycerol.

*To whom correspondence should be addressed at Gezondheidslei 96, 2930 Brasschaat, Belgium. E-mail: crowthers@compuserve.com

Copyright © 1998 by AOCS Press

analysis of octylphenoxypoly(ethoxy)ethanol. Extracted ion chromatograms were used for mass calibration rather than relying on external calibrants such as polystyrene. The uncertainty regarding use of the average mass spectrum for MW distribution was noted since this may be affected by instrumental parameters. Hunt, Binns, and Sheil (9) reported on the characterization of polyester resins by ESI/MS. Solvents, skimmer potential, and adduct ion were varied to produce an optimum ion current. M_n, M_w, and polydispersity were calculated from "optimum" conditions, but they were not validated. In a very recent article, Hunt *et al*. (10) provided a mathematical description on the effects of cone potential on the relative intensities of oligomer molecular ions. The magnitude of such effects on calculated M_n and M_w distributions for polyesters and poly(ethyleneglycol) is assessed. McEwen *et al*. (11) investigated concerns when calculating distribution information from mass spectra with multiple charged species and developed a program to transform ESI/MS spectra of synthetic polymers.

The difficulty in quantitating such complex analytes is apparent in several other reports. Duffin *et al.* (12) reported that the response factors of acylglycerols in ESI/MS analysis were dependent upon relative polarity. Byrdwell *et al.* (13) analyzed triacylglycerols using atmospheric pressure chemical ionization (APCI)/MS. After trying several approaches, the distribution of triacylglycerols with mixed fatty acid substitution was best represented when calculated response factors were used as opposed to actual response factors from a complex mixture of standard compounds. As Byrdwell *et al.* (13) point out, a synthetic mixture of standards was not useful for samples of disparate composition since the relative response factors are composition-dependent. For instance, we observed that the MW distribution of a polyglycerol can be quite different using flow injection method (vs. HPLC) since species of all MW are entering the ion source simultaneously. In addition, standards for a polyglycerol would be very difficult or even impossible to obtain. Evans *et al.* (14) utilized a deuterated internal standard blend ($C_{13}D_{17}O(EO)_xH$, ave. $x = 9$) for the spike and recovery analysis of an ethoxylated fatty alcohol (C_{12}–C_{15}) by ESI/MS. Response factors within the homologous alkyl series were assumed to be equivalent.

We used a nontraditional means to "validate" the distributions for the different polyglycerol products analyzed by LC–MS. The MW distributions obtained for each combination of cone voltage and adduct ion used in the analysis were judged by comparing the calculated OH# and cyclic content to actual values obtained by wet chemistry and GC, respectively. This is more akin to a chemometric solution where a spectrum is correlated to a bulk property (such as OH#) rather than by the traditional use of standard compounds. Once the best analysis conditions are obtained for the product type, the distribution from electrospray ionization (ESI)/MS can be used to calculate a number of characteristics. In addition, the observations on the effects of cone voltage and adduct ion on the electrospray response, and the observed distribution, emphasize considerations important to any analysis using ESI/MS.

EXPERIMENTAL PROCEDURES

Materials. Typical triglycerol, hexaglycerol, and decaglycerol samples were commercial materials (Lonza, Inc., Williamsport, PA). These samples had dry basis OH# of 1152, 960, and 881 which, for purely linear oligomers, represents an average degree of polymerization (n_{ave}) of 3, 6, and 10, respectively. All solvents used were HPLC grade (Mallinckrodt Chemical Inc., Chesterfield, MI). Deionized house water was filtered through a Millipore filter system (Millipore Corp., Bedford, MA) to 10 ohms. Mobile phases were degassed with helium sparging for approximately 10 min. The following compounds were purchased from Aldrich Chemical Co., Inc. (Milwaukee, WI): cesium acetate (99.995%); rubidium acetate (99.8%); potassium acetate (99.98%); sodium acetate (99.995%); and ammonium acetate (99+%). The acetic acid (glacial, 99.5%) was purchased from Mallinckrodt Chemical Inc.

OH# determination. OH# was determined according to AOAC official method of analysis 968.32 (15).

Water determination. The percentage of water was determined by a Karl Fischer titration (16).

GC. For the analysis of cyclic polymer content, the polyglycerol samples were acetylated with acetic anhydride. About 25 mg of sample was dissolved in 1 mL pyridine. The sample solution was mixed with 1 mL of acetic anhydride, evaporated to dryness (~60°C with N_2 stream), and the residue dissolved in about 1 mL methanol for analysis by GC. Samples were analyzed using an HP5890 (Hewlett-Packard Co., Palo Alto, CA) gas chromatograph equipped with an HP-7673A autosampler, a DB5-HT (J&W Scientific, Folsom, CA) 30 m × 0.32 mm i.d. capillary column, flame-ionization detector, and helium carrier gas (20 cm/s). One microliter of sample was injected with a 50:1 split. The injector port temperature was 280°C. Column temperature was ramped from 130 to 340°C at a rate of 8°C/min. The detector temperature was 350°C.

Since glycerol is not observed by ESI/MS, the percentage glycerol in the polyglycerol samples was determined by GC. A SPB-5 capillary column of 30 m × 0.32 i d (Supelco Inc., Bellefonte, PA) was used with an otherwise identical GC system as above. An internal standard calibration was used with propylene glycol as the internal standard. The silylated derivatives of glycerol and the polyglycerol samples were prepared for the analysis using bis(trimethylsilyl)-trifluoroacetamide (BSTFA) (Supelco Inc.). The injector port temperature was 275°C. One microliter of sample was injected with a 50:1 split. Column temperature was ramped from 70 to 320°C at a rate of 15°C/min. The detector temperature was 300°C.

HPLC-ESI/MS. The HPLC system consisted of a Hewlett-Packard HP1050 autosampler and pump. A HPX-87H ion exclusion column (BioRad Laboratories, Hercules, CA) with dimensions 30 cm × 7.8 mm was used with 1 mL/min mobile

phase flow rate. The column was heated to 60°C with an Eppendorf (Madison, WI) CH-30 heater. Polyglycerol samples were prepared as 0.1% solutions in mobile phase (50:50 acetonitrile/water). Fifty microliters of sample solution were injected. The separation was isocratic. A post-column addition of 1 mM solution of adduct ion in mobile phase was added at 0.4 mL/min using a Shimadzu (Columbia, MD) AD-10 pump and a zero-volume tee connector. The flow was then split approximately 50:1 with another tee connector. The larger volume flowed to a Waters (Milford, MA) 410 Differential Refractometer maintained at 50°C. The smaller volume was ntroduced into the electrospray source of the mass spectrometer at approximately 20 μL/min. A Platform II mass spectrometer from Micomass, Inc. (Beverly, MA) equipped with an electrospray source and probe was used. The electrospray source was maintained at 60°C. The probe capillary voltage was 3.5 kV, counter electrode (0.25 kV), cone voltage (varied from 30 to 100 V), skimmer lens offset (5 V), ion energy (IE) 1.0 V, and low mass (LM) and high mass (HM) resolution at 15 and 16 (arbitrary units), respectively. The nitrogen nebulizer gas was set at 10 L/h and drying gas approximately 250 L/h.

A mass calibration was routinely performed (with the same LM, HM, and IE values) using NaI/CsI solution from mass 150 to 1600 Dalton (*m/z*). Less than unit resolution was typically achieved across the mass range with mass errors less than 0.2 *m/z*.

Mass spectra were collected from 90 to 160 *m/z* to 1150 *m/z* with a scan time of 3.5 s, interscan time of 0.2 s and 8 data points per *m/z*. The total ion chromatogram was recorded over a 20-min elution time in the continuum mode. A mass spectrum was produced from co-adding spectra across the total elution time of the sample and subtracting co-added spectra from the background. Peak widths were relatively constant (0.6 amu) over the mass range. The result was smoothed and converted to centroid data.

Calculations. A sum of the A and A + 1 percentage base peak intensities for each observed ion were input into an Excel™ spreadsheet. The only other input to the spreadsheet was the wet basis OH#, and the wt% water and glycerol. From this, the following values were calculated: M_n, M_w, polydispersity, % cyclics, dry basis OH#, and wt% above $n = 6$.

RESULTS AND DISCUSSION

Data presentation overview. Two-dimensional map. Figure 2 shows a two-dimensional map of the HPLC-ESI/MS spec-

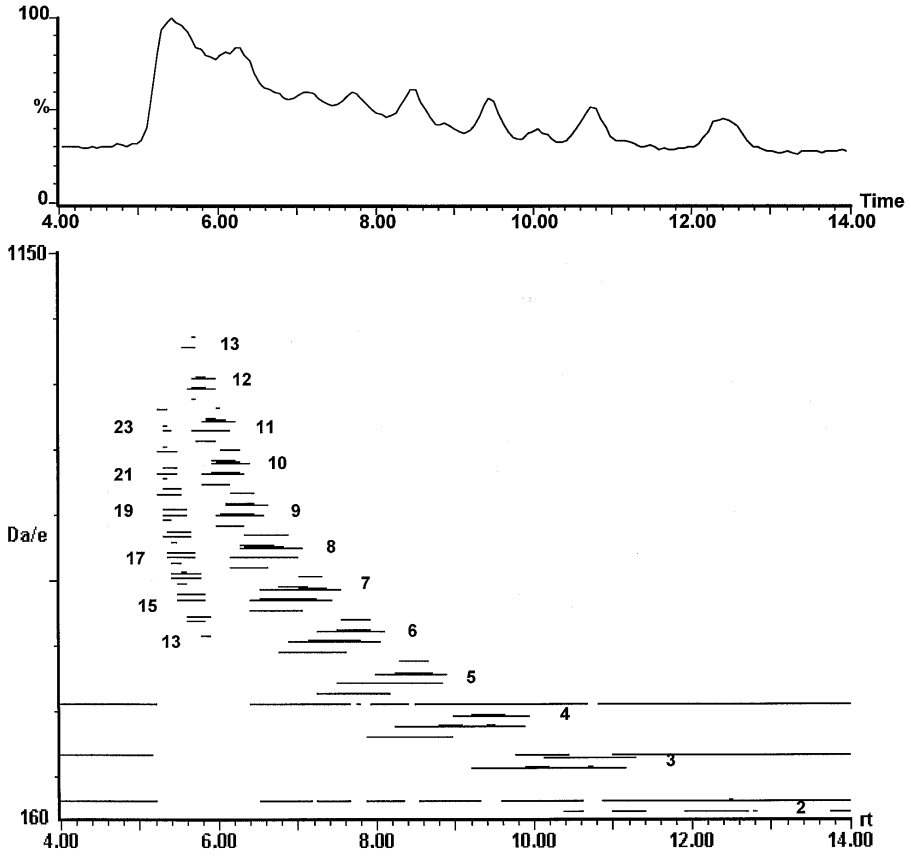

FIG. 2. Two-dimensional map of the high-performance liquid-chromatography–electrospray/mass spectrometry spectrum for the decaglycerol product (Na^+ adducts, cone voltage = 60). The profile on top is the reconstructed total ion current chromatogram. Each increasing degree of polymerization (*n*) is labeled from 2 to 13 and every other from 13 to 23.

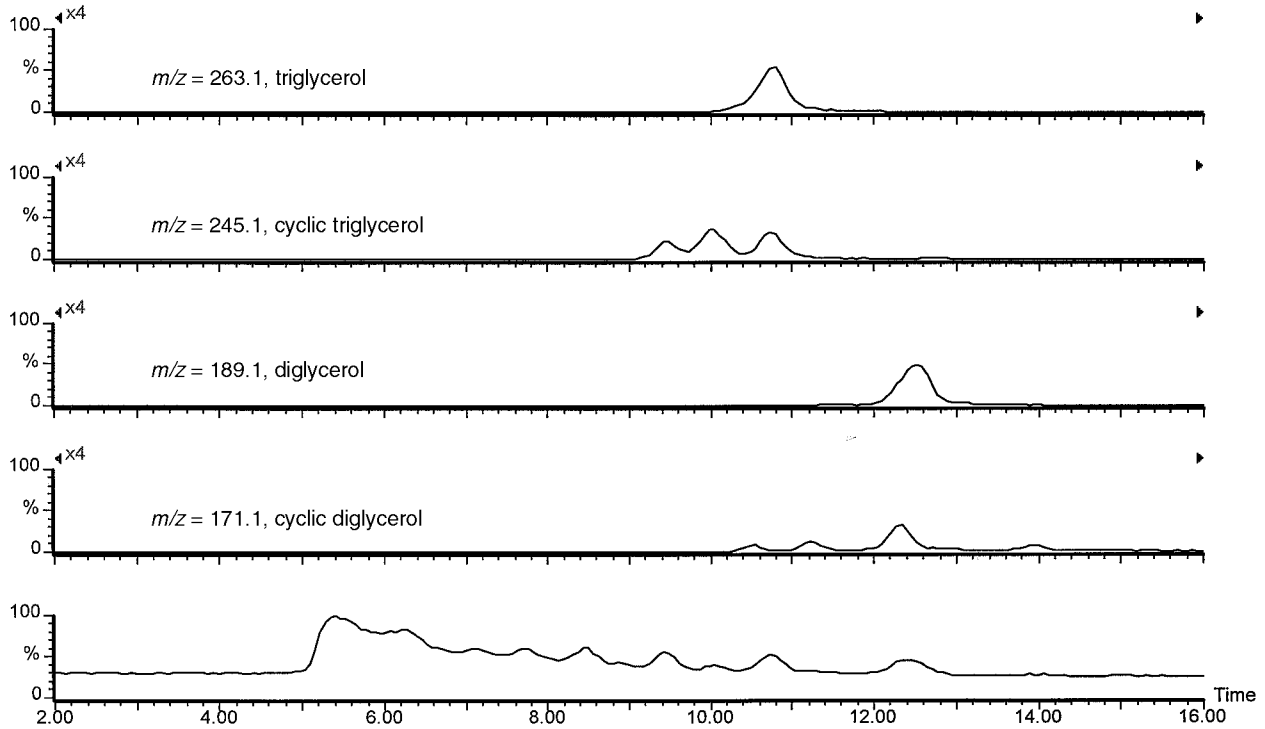

FIG. 3. Extracted ion chromatograms are displayed above the reconstructed total ion current chromatogram for the decaglycerol product (Na^+ adducts, cone voltage = 60).

trum obtained for the decaglycerol product (Na^+ adducts, cone voltage = 60). The mass axis provides resolution despite coelution. The two-dimensional map conveys the complete composition at a glance. Linear and cyclic polymers with the same degree of polymerization appeared at approximately the same retention time, starting with $n = 2$ at 12.5 min and trending upward in mass to $n = 13$ at approximately 6 min. Higher mass or longer chain polymers were observed coeluting under 6 min. These are multiply charged ions of polymers ($[M + 2Na]^{+2}$) at half-*m/z* starting toward the bottom of the plot with $n = 13$ at 513.23 *m/z* {*m/z* = [980.49 + (2 × 22.99)]/2} up to $n = 23$ at 883.42 *m/z* {*m/z* = [1720.86 + (2 × 22.99)]/2}. Multiple ion adducts of sodium with other polyols, specifically poly(ethylene glycol)s, have been noted before (17). Each group at a single degree of polymerization also displayed cyclic components at slightly shorter retention times and successions of 18 *m/z* below the linear chain for the loss of water. The cyclic products for chains with $n > 12$ are also multiply charged and appeared at 9 *m/z* decrements from the linear chain polymer ions. The lines across the bottom of the plot are sodium acetate clusters $[Na_{n+1}(OAc)_n]$ that elute continuously. Occasionally, clusters were observed for small (n = 2~4) polyglycerol oligomers too. These eluted at the same retention time as the nonclustered ion (e.g., 12.5 min for $n = 2$, $[1\ M_{n=2} + Na]^{+1}$) but at multiple masses (e.g., $[2\ M_{n=2} + Na]^{+1}$, $[3\ M_{n=2} + Na]^{+1}$, etc.).

Extracted ion chromatograms. Extracted ion plots can convey additional information not easily observable in the two-dimensional display. Now, one can see resolution on the time axis in spite of mass overlap. For instance, cyclic isomers of di- and triglycerol that have the same mass were chromatographically resolved as observed in the extracted ion plot (Fig. 3).

Mass spectrum. The mass spectra co-added across the total elution volume of the sample, or a summed projection of the two-dimensional map on the mass axis, provide the total mass distribution of the sample (Fig. 4). Each successive degree of polymerization is labeled at the mass for the linear (or branched) chains. Cyclic isomers appear at −18 *m/z* decrements from the linear mass. The next phase of this study addresses whether this distribution represents the true sample composition. Rather different distributions can be obtained for the same sample with variations in cone voltage and adduct ion, all other parameters remaining constant. This is particularly true for the higher MW products.

EFFECTS OF CONE VOLTAGE AND ADDUCT ION

HPLC-ESI/MS was performed for tri-, hexa-, and decaglycerol products with every adduct cation (H^+, Li^+, Na^+, K^+, Rb^+, Cs^+, and NH_4^+) at cone voltages 30, 40, 60, 80, and 100. Results from every combination of adduct ion and cone voltage were input into the spreadsheet. The OH# and % cyclics were computed and compared to the values obtained from wet chemistry and GC, respectively. The observed effects of cone voltage and adduct ion are noteworthy. While adducts of other polyols with Na^+, K^+ and NH_4^+ have been noted before, a sys-

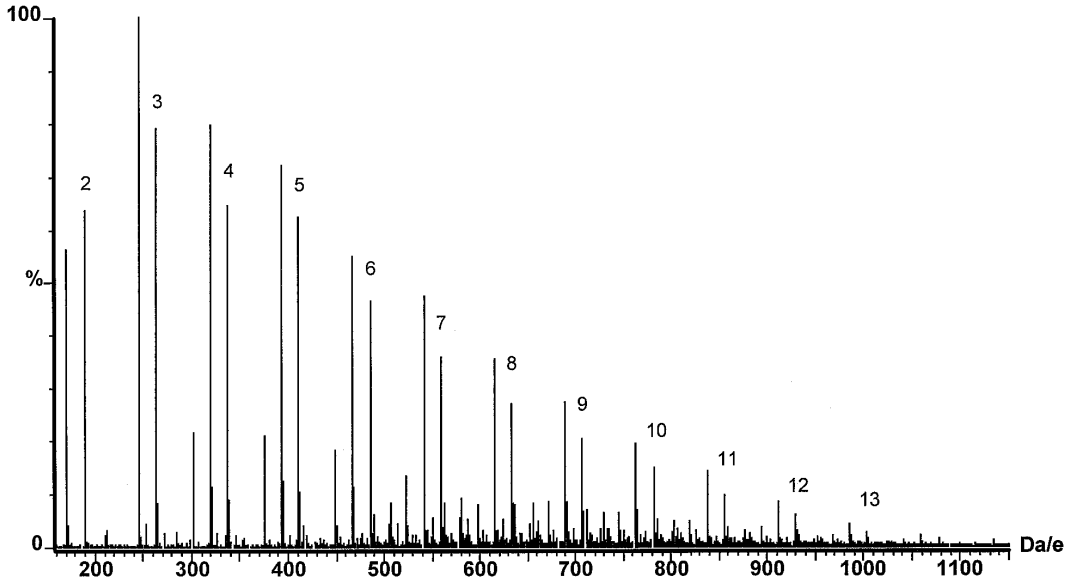

FIG. 4. The mass spectrum summed over the total elution time for the decaglycerol product (Na^+ adducts, cone voltage = 60).

tematic study of the effects on the MW distribution and dependence with cone voltage has not been elaborated. Several authors have noted the increased stability of Na^+ adducts (9,12,14,18). Tang and Kerbarle (19) have given a theoretical description of the electrospray response for many cations by themselves (not adduct species).

Figures 5 and 6 show Na^+ adducts ($[M + nNa]^{+n}$) of triglycerol and decaglycerol products at cone voltages equal to 30, 40, 60, 80, and 100V. First of all, there are obvious differences between the products that are not evidenced by GC or LC alone. At any cone voltage, the biggest difference between the triglycerol and decaglycerol products was the proportion of cyclic material. For the decaglycerol product, the cyclic structures (at −18 *m/z*, H_2O) were as large as or larger

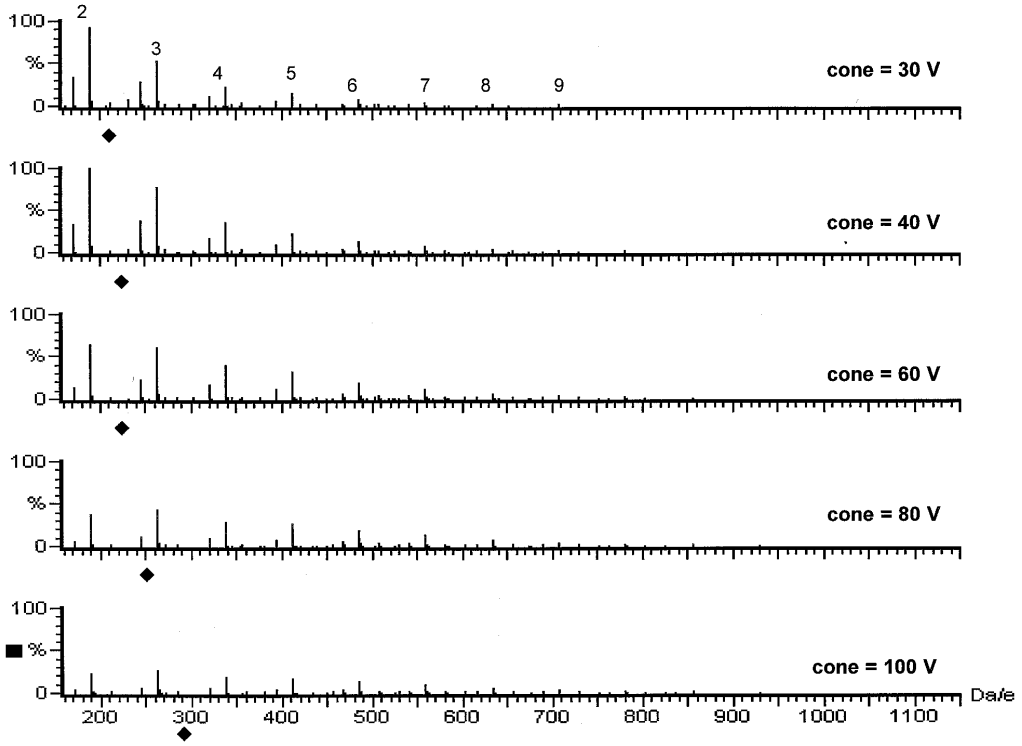

FIG. 5. The effect of cone voltage on the observed mass distribution for the triglycerol, Na^+ adducts, product. The diamonds indicate the center of mass (n_{ave}) in each spectrum.

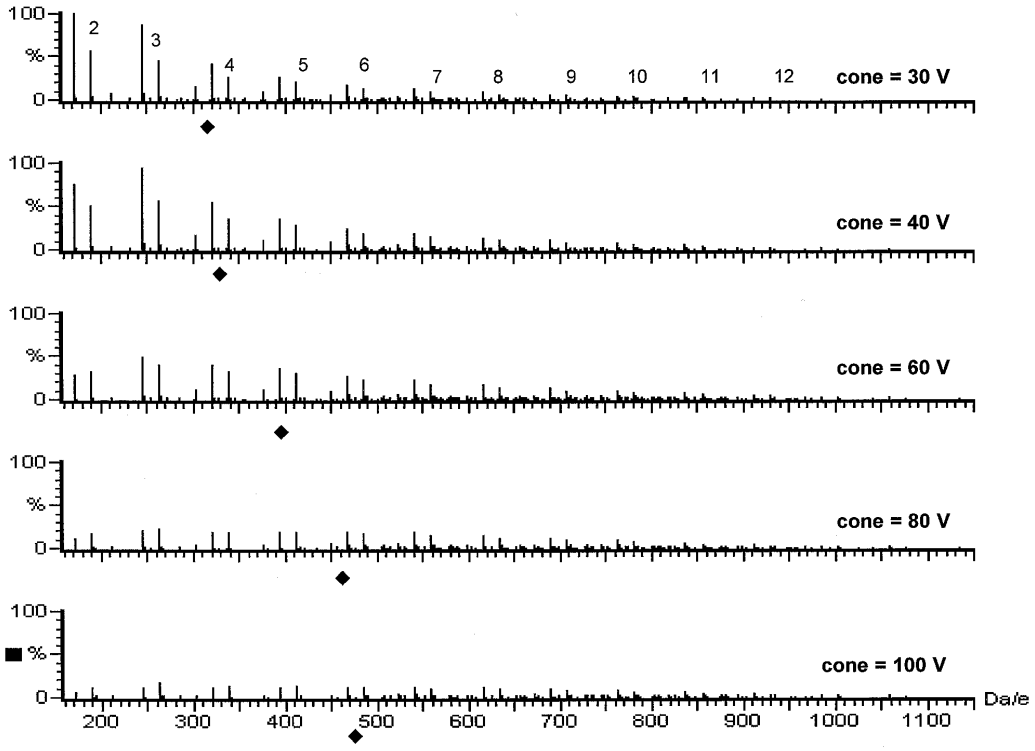

FIG. 6. The effect of cone voltage on the observed mass distribution for the decaglycerol, Na^+ adducts, product. The diamonds indicate the center of mass (n_{ave}) in each spectrum.

than the linear oligomers at any degree of polymerization (n). In addition, the decaglycerol product had a significant amount of dicyclic structures (at −36 *m/z*, $2H_2O$). The decaglycerol product distribution centers about a mass that was only 1.5–2.5 polymer units higher than that for the triglycerol product. This center of mass, designated by diamonds in the figures, increased with increasing cone voltage. This effect has been noted before and can be attributed to improved focusing for the higher mass ions at higher cone potentials (10). The effect is greater for the decaglycerol product since higher MW components are more abundant but are not as evident until the higher cone voltages are used. The average degree of polymerization (n_{ave}) for the decaglycerol product increased from 3.6 at a cone voltage of 30 to 5.8 at a cone voltage of 100. For the triglycerol product, the n_{ave} increased from 2.2 to 3.3 over the same range of cone voltage. The spectra in Figures 5 and 6 are plotted on the same vertical scale. At a cone voltage of approximately 60 (or higher), charge stripping (10,11,20,21) began as evidenced by the increased drop in the total ion current intensity. Fragmentation of the polymer molecule itself is also possible but was not observed here. The small oligomers (n = 2,3) seem the most susceptible to charge stripping, especially the cyclic oligomers. The smaller ions dissociate first since they have more internal energy, which is inversely related to mass (10). Also, they have fewer oxygen atoms with which to bond to the adduct ion with and hence are more loosely associated to begin with.

Figure 7 shows the decaglycerol product with the adduct series, H^+, Li^+, Na^+, K^+, Rb^+, and Cs^+ with a constant cone voltage setting of 40 V. A plot for the NH_4^+ adduct is omitted since, as has been noted before (12), the ammonium ion fragments to ammonia and produces, in this case, predominantly protonated adducts. The spectra are plotted with the same vertical scale. An expansion is noted by the number in the upper left corner. The most stable adducts are formed with either Li^+ or Na^+ which have the highest total ion current. Adducts with H^+, K^+, Rb^+, and Cs^+ were relatively unstable as indicated by the lower total ion currents. The n_{ave} showed a significant increment with an increase in adduct size. For triglycerol, n_{ave} moved from 2.5 ± 0.1 for H^+, Li^+, and Na^+ to 3.1 ± 0.1 for K^+, Rb^+, and Cs^+. For decaglycerol, n_{ave} jumped from 3.8 ± 0.1 for H^+, Li^+, and Na^+ to 5.2 ± 0.2 for K^+, Rb^+, and Cs^+. Glycerol did not form a stable adduct with any ion and was never observed. Therefore, the first observed adduct in every series was the cyclic diglycerol. Hardly any cyclic diglycerol adduct was observed with the too large Rb^+ and Cs^+ ions. Although the K^+ and Cs^+ adducts are less stable than Na^+, they favored the heavier polymer chains which is important for higher degrees of polymerization. In addition, polyglycerol molecules with multiple adduct ions that occur with polymer chains with $n > 13$ were reduced with Cs^+ ions. This is exhibited in Figure 8 that shows an overlay of a small region of the spectrum of the decaglycerol product with Na^+ (cone = 40 V) and Cs^+ adducts (cone = 30 V). The circles represent high chain polymers with two adduct ions that ap-

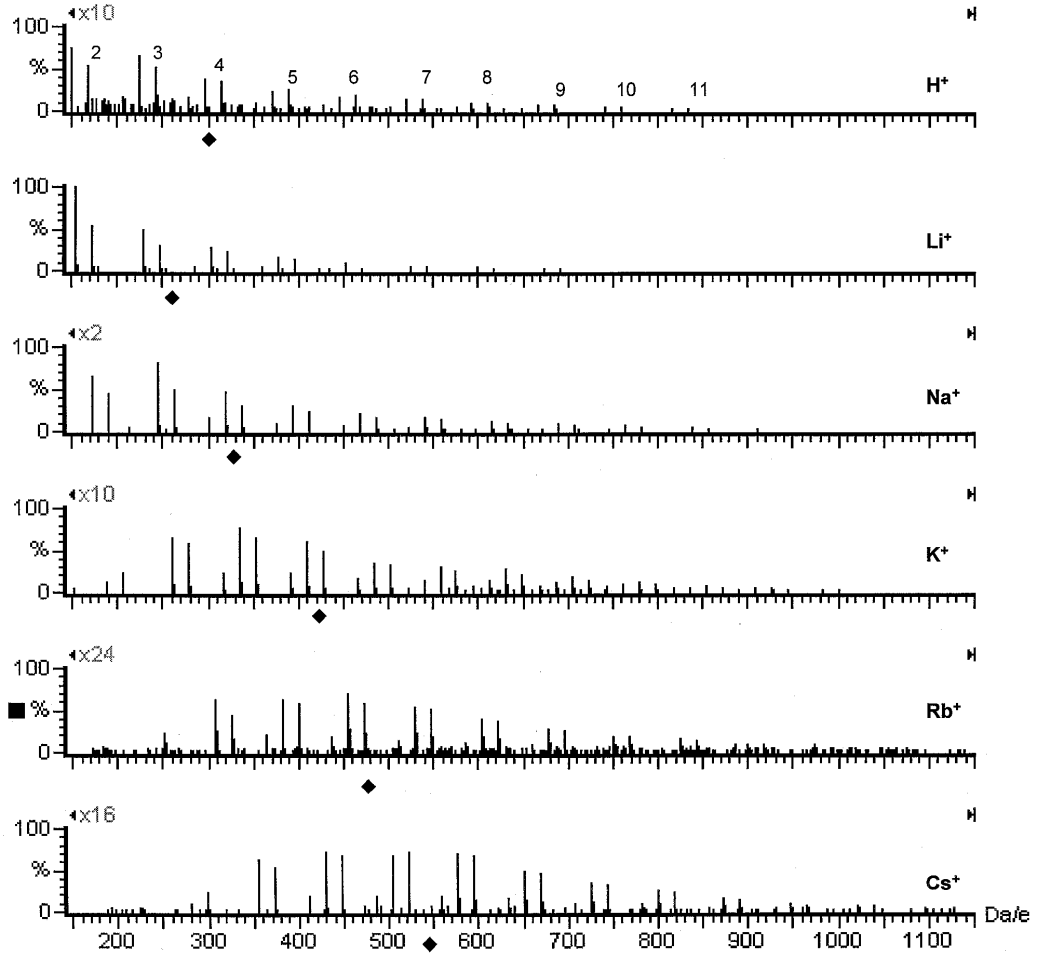

FIG. 7. The effect of adduct ion on the observed mass distribution for the decaglycerol product. Cone = 40. The diamonds indicate the center of mass (n_{ave}) in each spectrum.

peared at half-mass. Of course, the ion currents optimized at different cone potentials for the different adduct ions.

DETERMINATION OF THE BEST DISTRIBUTION

Since determination of the best (most representative) distribution is impractical by use of standard materials, we chose to "reduce" the data to two numerical values representing bulk sample properties that can be checked by independent experimental means. A combination of the OH# that is sensitive to both the degree of polymerization and the % cyclics, and a % cyclics estimated from GC analysis was used. The quoted range for wt% cyclics given by GC is the range of relative peak area of cyclic to linear polymer for all degrees of polymerization observed. For example, for the triglycerol product, the % cyclic at $n = 2$ is 18% and 11% at $n = 6$ which is the highest degree of polymerization observed. Glycerol is not observed by ESI/MS and therefore had to be determined by GC. The percentage glycerol was included in the spreadsheet calculations since it can have a significant contribution to OH#, M_n, etc. Table 1 summarizes the wet chemistry and GC results.

An Excel™ spreadsheet was used to calculate the OH#, % cyclics, M_n, M_w, polydispersity, and the percentage above hexad from the ion intensities observed in the mass spectra. Tables 2–4 summarize the calculated OH# and the % cyclic obtained for each product for all the analysis combinations of cone voltage and adduct ion. The shaded areas are combinations that give good agreement to the GC and wet chemistry results. There may be more than one suitable combination that provides a distribution within reasonable error. The final analysis conditions chosen, underlined in bold type, were favored for reasons given in the discussion on the effect of cone voltage and adduct ion. The choice of ammonium as an

TABLE 1
Wet Chemistry and GC Results[a]

Sample ID/test	Wet OH#	Dry OH#	% water	% glycerin (GC)	% cyclic (GC)
Triglycerol	930	1152	19.3	11.67	11–18
Hexaglycerol	794	960	17.3	3.39	28–38
Decaglycerol	719	881	18.4	2.05	34–51

[a]GC, gas chromatography; OH#, hydroxyl number.

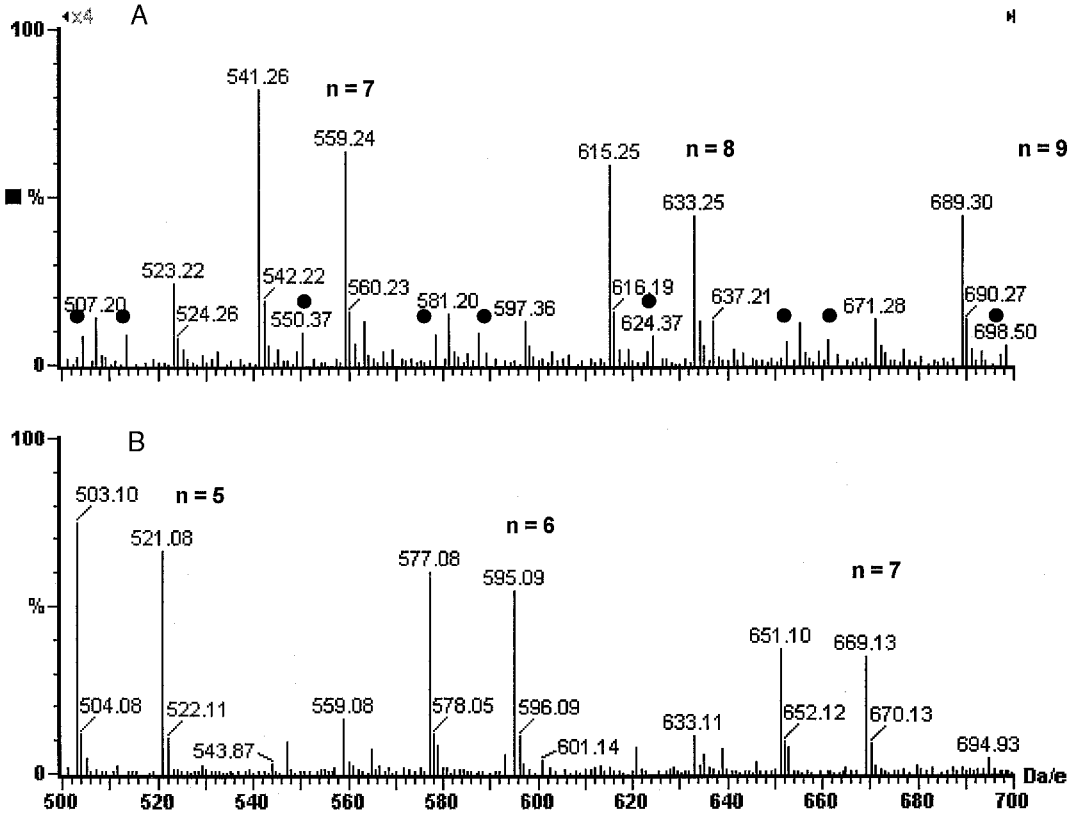

FIG. 8. (A) The mass spectrum for the decaglycerol product with Na^+ adducts at a cone voltage = 40 V. (B) The mass spectrum for the decaglycerol product with Cs^+ adducts at a cone voltage = 30 V. Multiple-charged high mass polymer chains ($[M + 2\ Na]^{+2}$) that appear at half-mass are noted in the top spectrum with filled circles.

adduct was eliminated because of the extensive fragmentation of the NH_4^+ ion. Figure 9 shows the combined mass spectrum over the total elution volume using the preferred analysis conditions for each product. Table 5 gives the final conditions for each product and the important parameters calculated from the obtained mass distribution. Again, the most stark contrast between products is not the degree of polymerization (M_n or M_w) but the proportion of cyclic material.

Table 6 compares calculations of the OH# and % cyclic from the ESI/MS distribution to that obtained by GC/flame-ionization detector and HPLC/RI for the triglycerol product. Even for this simplest product, the OH# calculated from the

TABLE 2
Triglycerol Product[a]

Adduct/ cone	H^+	LI^+	Na^+	K^+	Rb^+	Cs^+
30	1116	**1152**	1135	1083	1105	1085
	21	**21**	26	26	21	21
40	1096	1145	1119	1056	1084	1021
	23	21	24	25	19	18
60	1086	1137	1097	1037	1066	1046
	22	21	21	23	19	20
80	1091	1128	1083	1045	1058	1043
	21	20	18	19	14	16
100	1041	1096	1071	1029	1048	1029
	28	20	18	22	15	18

[a]Validation specifications: dry basis OH# = **1152**; cyclics (GC) = **11–18**. The shaded areas are combinations that give good agreement to the GC and wet chemistry results. There may be more than one suitable combination that provides a distribution within reasonable error. The final analysis conditions chosen are underlined in bold type. For abbreviations see Table 1. The top and bottom number for each adduct/cone pair is the calculated OH# and % cyclic value, respectively.

TABLE 3
Hexaglycerol Product[a]

Adduct/ cone	H^+	LI^+	Na^+	K^+	Rb^+	Cs^+
30	960	**961**	928	895	919	897
	46	**48**	53	50	44	44
40	918	**949**	916	881	906	876
	47	**48**	52	50	42	46
60	888	941	903	880	901	857
	47	47	48	49	39	46
80	897	942	908	877	885	840
	45	42	43	48	42	48
100	908	927	915	882	889	848
	42	45	39	47	43	51

[a]Validation specifications: dry basis OH# = **960**; cyclics (GC) = **28–38**. For abbreviations see Table 1. See Table 2 footnote for explanation of bold numbers, shaded areas, and adduct/cone pair.

TABLE 4
Decaglycerol Product[a]

Adduct/ cone	H^+	LI^+	Na^+	K^+	Rb^+	Cs^+
30	905	899	869	849	862	859
	52	61	62	61	56	55
40	886	898	**870**	833	858	854
	52	60	**61**	61	55	55
60	878	892	860	827	854	844
	51	57	57	60	53	54
80	878	875	840	822	884	835
	49	56	58	61	47	54
100	869	888	850	820	892	837
	50	53	56	62	42	53

[a]Validation specifications: dry basis OH# = **881**; cyclics (GC) = **34–51**. For abbreviations see Table 1. See Table 2 footnote for explanation of bold numbers, shaded areas, and adduct/cone pair.

TABLE 5
Calculated Values for the Triglycerol Product Li^+, Hexaglycerol Product Li^+ and Decaglycerol Product Na^+ Adducts[a]

	Triglycerol product Li^+ adducts cone voltage = 30	Hexaglycerol product Li^+ adducts cone voltage = 40	Decaglycerol product Na^+ adducts cone voltage = 40
OH#	1152	949	870
M_n	193	254	299
	n_{ave} = 2.4	n_{ave} = 3.2	n_{ave} = 3.8
M_w	306	367	399
Polydispersity	1.59	1.44	1.34
wt% cyclics	21	48	61
wt% >hexa	7.6	24	29

[a]Abbreviations: M_n, number average molecular weight; M_w, weight average molecular weight; OH#, hydroxyl number.

TABLE 6
Calculated Values for the Triglycerol Product[a]

	OH# (wet-1152)	wt% cyclics
GC	1304	1118
HPLC/RI	1290	0
HPLC–ESI/MS	1152	21

[a]From distributions obtained by GC, HPLC/RI, and HPLC–ESI/MS analysis. HPLC/RI, high-performance liquid chromatography–refractive index (RI); HPLC–ESI/MS, HPLC–electrospray/mass spectrometry. See Tables 1 and 5 for other abbreviations.

GC and HPLC/RI distributions are different than the wet chemistry value by ~150 hydroxyl number units. The GC distribution is in error since the intensities are progressively suppressed for each degree of polymerization. ESI/MS shows that the proportion of cyclic material increases with increasing degree of polymerization. GC actually shows the opposite trend. This and the fact that higher degrees of polymerization are increasingly attenuated in GC explains why the % cyclic by ESI/MS is always biased high. The HPLC distribution is in error since no cyclic components are resolved or accounted for.

ACKNOWLEDGMENTS

The authors wish to acknowledge Jonathan Crowther and David Peake for very helpful discussions during the course of this work. The spreadsheet that was developed to calculate the OH#, M_n, M_w, polydispersity, etc., from the observed molecular ions in the averaged mass spectrum and the percentage water and glycerol can be made available to interested persons by contacting Dr. Stephen P. Carter at Lonza, Inc.

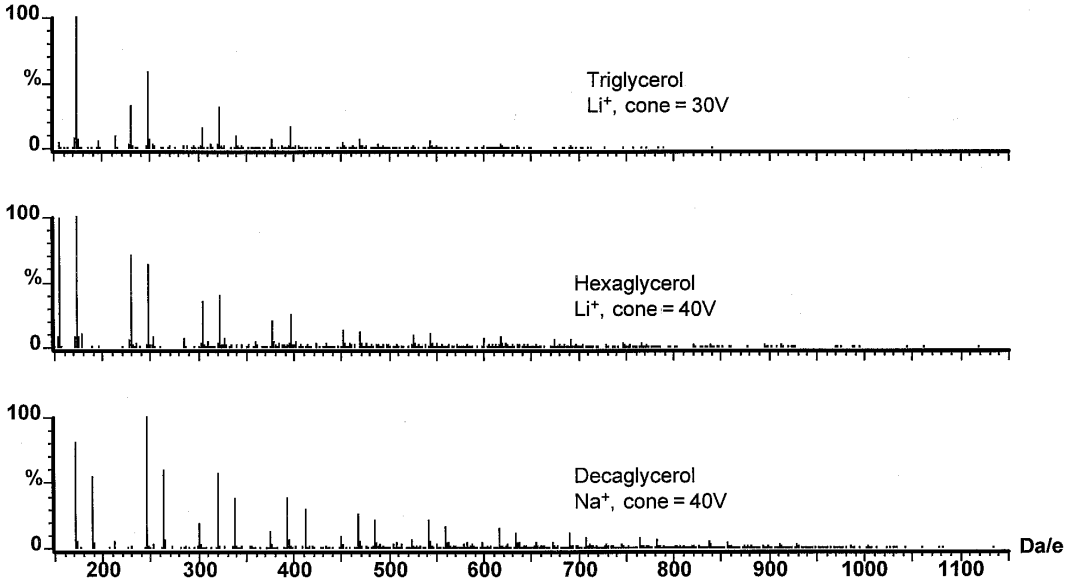

FIG. 9. The most representative mass distribution for each product is displayed. Tables 2–4 give values for parameters calculated from these spectra.

REFERENCES

1. Sen, N., M. Keating, and C.B. Barrett, Gas–Liquid Chromatography of Polyglycerol, *J. Gas Chromatogr. 5*:269–270 (1967).
2. Kumar, T.N., Y.S.R. Sastry , and G. Lakshminarayana, Analysis of Polyglycerols by High-Performance Liquid Chromatography, *J. Chromatogr. 298*:360–365 (1984).
3. Macka, M., H.-P. Mettler, M. Bokel, and W. Roder Analysis of Silanised Polyglycerols by Supercritical Fluid Chromatography, *J. Chromatogr. A 675*:267–270 (1994).
4. Stenzel, W.R., and C.L. Franzke, Zur Kenntnis der Polyglycerinfettsaureester, *Die Nahrung, 21(5)*:429–441 (1977).
5. Stenzel, W.-R., and F. Claus, Synthese und Anwendung von Polyglyzerin und Polyglyzerinfettsaureestern als Emulgatoren in der Lebensmittelindustrie, *Die Lebensmittel-Industrie 24*:503–506 (1977).
6. Dolhaine, V.H., W. Preuss, and K. Wollmann, Strukturen im "Polyglycerin," *Fette, Seifen, Anstrichmittel, 86(9)*:339–342 (1984).
7. Dolhaine, V.H., W. Preuss, and K. Wollmann, Structures in "Polyglycerol," *Henkel-Referate 21/Int. Ed.*:80–87 (1985).
8. Prokai, L., and W.J. Simonsick, Jr., Electrospray Ionization Mass Spectrometry Coupled with Size-Exclusion Chromatography, *Rapid Comm. Mass Spectrom 7*:853–856 (1993).
9. Hunt, S.M., M.R. Binns, and M.M. Sheil, Structural Characterization of Polyester Resins by Electrospray Mass Spectrometry, *J. Appl. Polym. Sci. 56*:1589–1597 (1995).
10. Hunt, S.M., M.M. Sheil, M. Belov, and P.J. Derrick, Probing the Effects of Cone Potential in the Electrospray Ion Source: Consequences for the Determination of Molecular Weight Distributions of Synthetic Polymers, *Anal. Chem. 70*:1812–1822 (1998).
11. McEwen, C.N., W.J. Simonsick, Jr., B.S. Larsen, K. Ute, and K. Hatada, The Fundamentals of Applying Electrospray Ionization Mass Spectrometry to Low Mass Poly(Methyl Methacrylate) Polymers, *J. Am. Soc. Mass Spectrom. 6*:906–911 (1995).
12. Duffin, K.L., J.D. Henion, and J.J. Shieh, Electrospray and Tandem Mass Spectrometric Characterization of Acylglycerol Mixtures That Are Dissolved in Nonpolar Solvents, *Anal. Chem. 63*:1781–1788 (1991).
13. Byrdwell, W.C., E.A. Emken, W.E. Neff, and R.O. Adlof, Quantitative Analysis of Triglycerides Using Atmospheric Pressure Chemical Ionization-Mass Spectrometry, *Lipids 31*: 919–935 (1996).
14. Evans, K.A., S.T. Dubey, L. Kravetz, W.W. Evetts, I. Dzidic, and C.C. Dooyema, Quantitation of Alcohol Ethoxylate Surfactants in Environmental Samples by Electrospray Mass Spectrometry, *J. Am. Oil Chem. Soc. 74*:765–773 (1997).
15. Association of Official Analytical Chemists, *AOAC Official Methods of Analysis,* Method 965.32, 1990.
16. Association of Official Analytical Chemists, *Ibid.,* Method 977.10, 1990.
17. Nohmi, T., and J.B. Fenn, Electrospray Mass Spectrometry of Poly(ethylene glycols) with Molecular Weights Up to Five Million, *J. Am. Chem. Soc. 114*:3241–3246 (1992).
18. Sherrard, K.B., P.J. Marriott, and M.J. McCormick, Electrospray Mass Spectrometric Analysis and Photocatalytic Degradation of Polyethoxylate Surfactants Used in Wool Scouring, *Anal. Chem. 66*:3394–3399 (1994).
19. Tang, L., and P. Kerbarle, Dependence of Ion Intensity in Electrospray Mass Spectrometry on the Concentration of the Analytes in the Electrosprayed Solution, *Ibid. 65*:3654–3668 (1993).
20. Cody, R.B., J. Tamura, and B.D. Musselman, Electrospray Ionization/Magnetic Sector Mass Spectrometry: Calibration, Resolution, and Accurate Mass Measurements, *Ibid. 64*:1561–1570 (1992).
21. Thomson, B.A., Declustering and Fragmentation of Protein Ions from an Electrospray Ion Source, *J. Am. Soc. Mass Spectrom. 8(10)*:1053–1058 (1997).

[Received November 11, 1997; accepted August 7, 1998]